



Optimization study of a muon tomography system for imaging of nuclear waste containers

A.Sh. Georgadze

Kiev Institute for Nuclear Research
Institute of Physics, University of Tartu

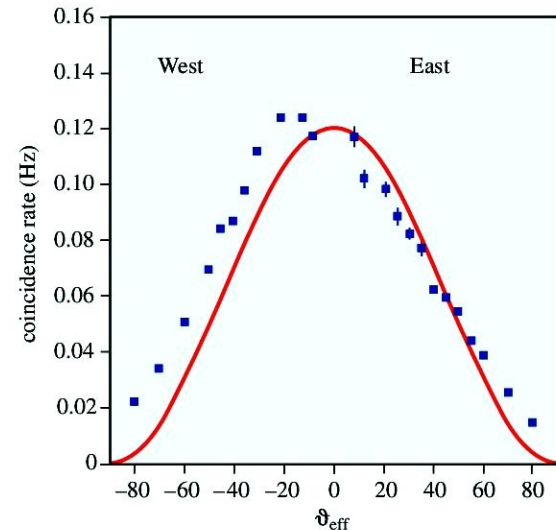
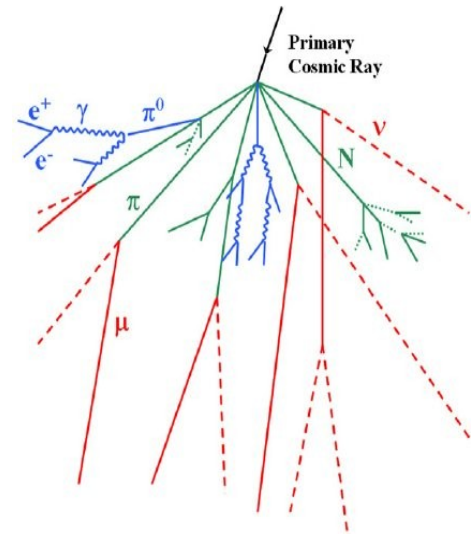
4-th Jagiellonian Symposium on Fundamental and Applied Subatomic Physics
Krakow, Poland, 2022

a.sh.georgadze@gmail.com

anzori.heorhadze@ut.ee

Cosmic rays: muons

- Primary cosmic rays, mainly protons, interact in the atmosphere and produce showers of secondary cosmic rays. Different particles in the shower are absorbed in atmosphere but since muons are the most penetrating they can reach a sea level.
- On Earth we are constantly bathed in muons, occurring at rates ~ 10000 muons/m²/sec.
- Large angular and energy spread.
- Highly penetrating.
- Flux and energy of muons depend on the zenith angle. Flux distribution of cosmic ray muons follow $\cos^2(\theta)$ law, where θ is angle of incidence. As a result, most of muons traversing muon detector comes from top and less from sides.



Conditioned radioactive waste characterization and quality control

- Nuclear industry have been and is producing waste. The existence of long-lived radio nuclides that have both radiotoxic and chemotoxic effects within these waste means that particular care and consideration must be taken when developing appropriate disposal methods.
- Conditioned nuclear waste is in steel containers inside concrete or bitumen matrices.
- There is a need for non-destructive techniques that will improve the characterization of conditioned radioactive waste using different techniques:
 - Calorimetry as a non-destructive technique to reduce uncertainties on the inventory of radio nuclides
 - Muon Tomography as a non-destructive technique to control the content of large volume nuclear waste
 - Cavity Ring-Down Spectroscopy to characterize outgassing of radioactive waste
 - Muon Tomography has been shown capability of characterization of nuclear waste.



Application of muon scattering tomography for waste drum imaging

$$\theta_0 = \frac{13.6\text{MeV}}{\beta c p} \cdot z \sqrt{\left(\frac{x}{X_0}\right)} \cdot \left[1 + 0.038 \ln\left(\frac{x}{X_0}\right)\right]$$

$\beta c \rightarrow$ Velocity

$p \rightarrow$ Momentum

$z \rightarrow$ Charge Number

$x \rightarrow$ Width of Medium

$X_0 \rightarrow$ Radiation Length

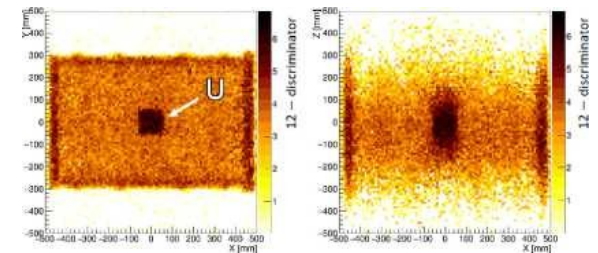
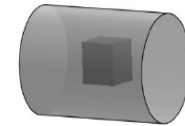
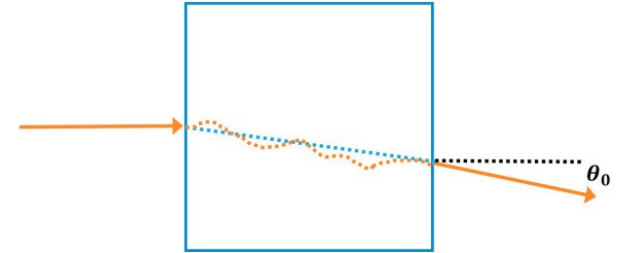
$$X_0 = \frac{716.4\text{g/cm}^2}{\rho} \frac{A}{Z(Z+1)\ln\left(\frac{287}{\sqrt{Z}}\right)}$$

Muon tomography relies on Coulomb multiple scattering of muons. The angular distribution is approximately Gaussian, with θ_0 depending on the radiation length X_0 and on Z .

The Z^2 means that the technique is very sensitive for high- Z materials.

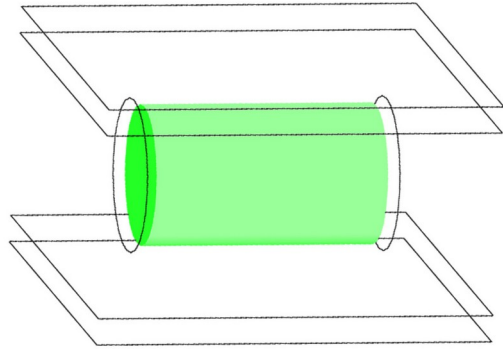
Muon scattering tomography allow to measure hit position in tracking detectors and reconstruction of the scattering angle

θ_0 .

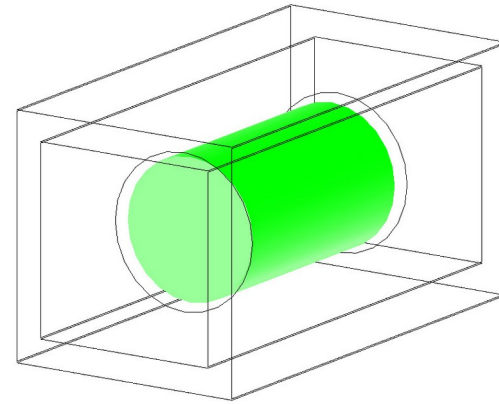


Imaging of nuclear waste drums using resistive plate chambers

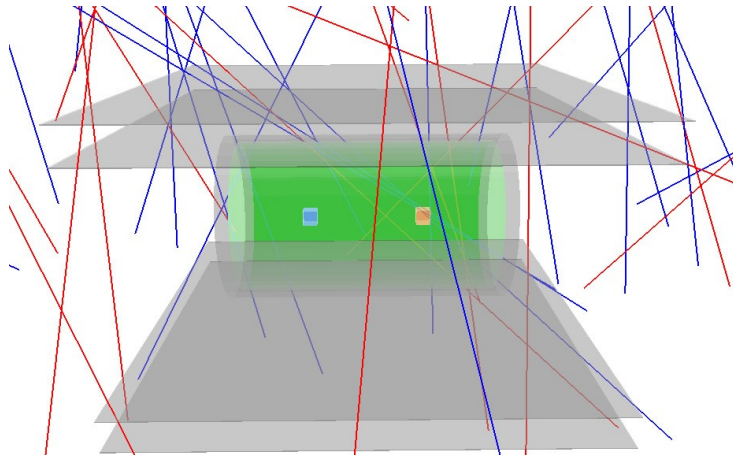
Simulation of two detector geometries using Geant4



1st detector scheme - planar detector type with 2 tracking detectors with size 150 cm x 150 cm on both sides of the waste drum



2nd detector scheme – tunnel type, such a geometry allow detect more inclined muons and better reconstruct Z coordinate of high-Z targets



Cosmic Ray Shower Library (CRY) interfaced with GEANT4 package used to simulate data samples with 60 minutes measurement time

Lead target

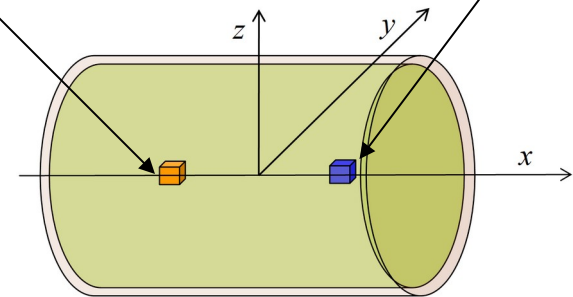
$Z = 82$

Density = 11.3 g/cm³

Tungsten target

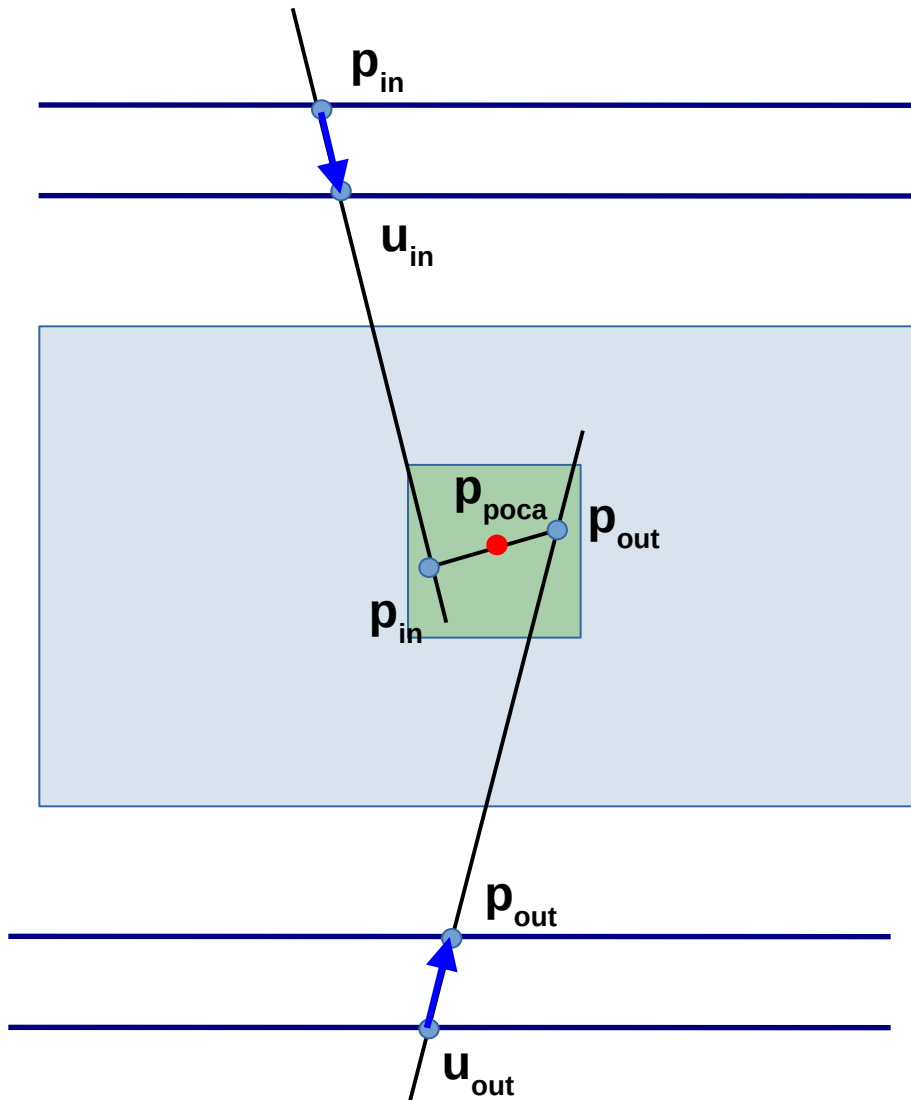
$Z = 74$

Density = 19.3 g/cm³



Concrete filled drum with conditioned nuclear waste with size $\varnothing 574$ mm x 960 mm

Image reconstruction using Point of Closest Approach algorithm



The Point of Closest Approach is a simplest approach, fast and easy to implement

Geometrical point of closest approach between incoming and outgoing tracks

To calculate the scattering angle between two tracks we use formula

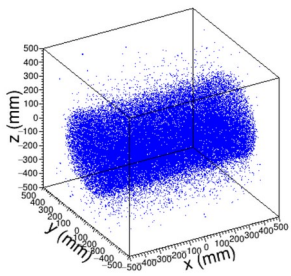
$$\theta_{scatt} = \arccos(\mathbf{v}_{in} \cdot \mathbf{v}_{out})$$

Spatial distribution of the scattering centers, weights given by some power of the scattering angle

To remove background from concrete matrix were implemented clustering algorithm and median filtering

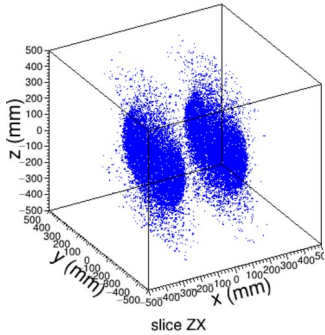
PoCA imaging of 5 cm³ tungsten and lead targets

3D PoCA cloud

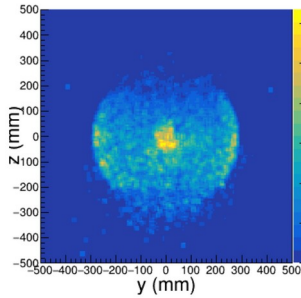


a) POCA reconstruction of the nuclear waste drum.

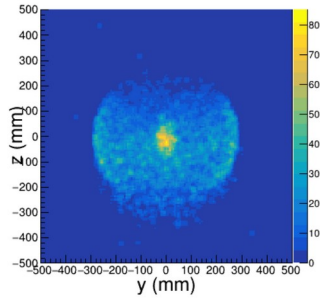
a)



slice ZY1 zy projection

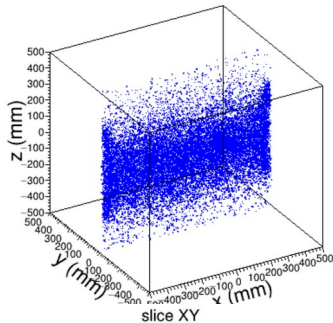


slice ZY2 zy projection

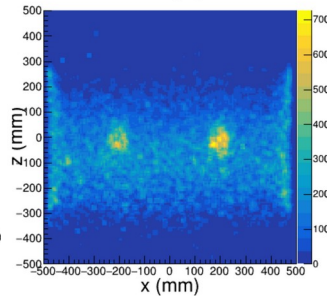


b) Two vertical 100 mm POCA slices of in the ZY plane centered at the locations $x = -20$ cm and $x = 20$ cm were tungsten and lead targets are placed are made to improve signal-to-noise ratio.

b)

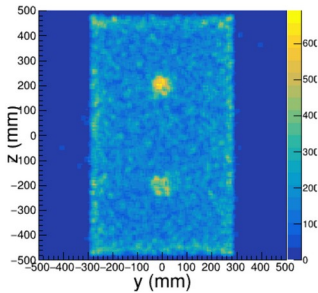
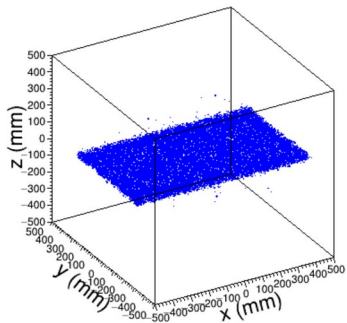


slice ZX zx projection



c) Vertical 100 mm slice of in the ZX plane centered at the locations $y = 0$ cm. were tungsten and lead targets are located to improve signal-to-noise ratio.

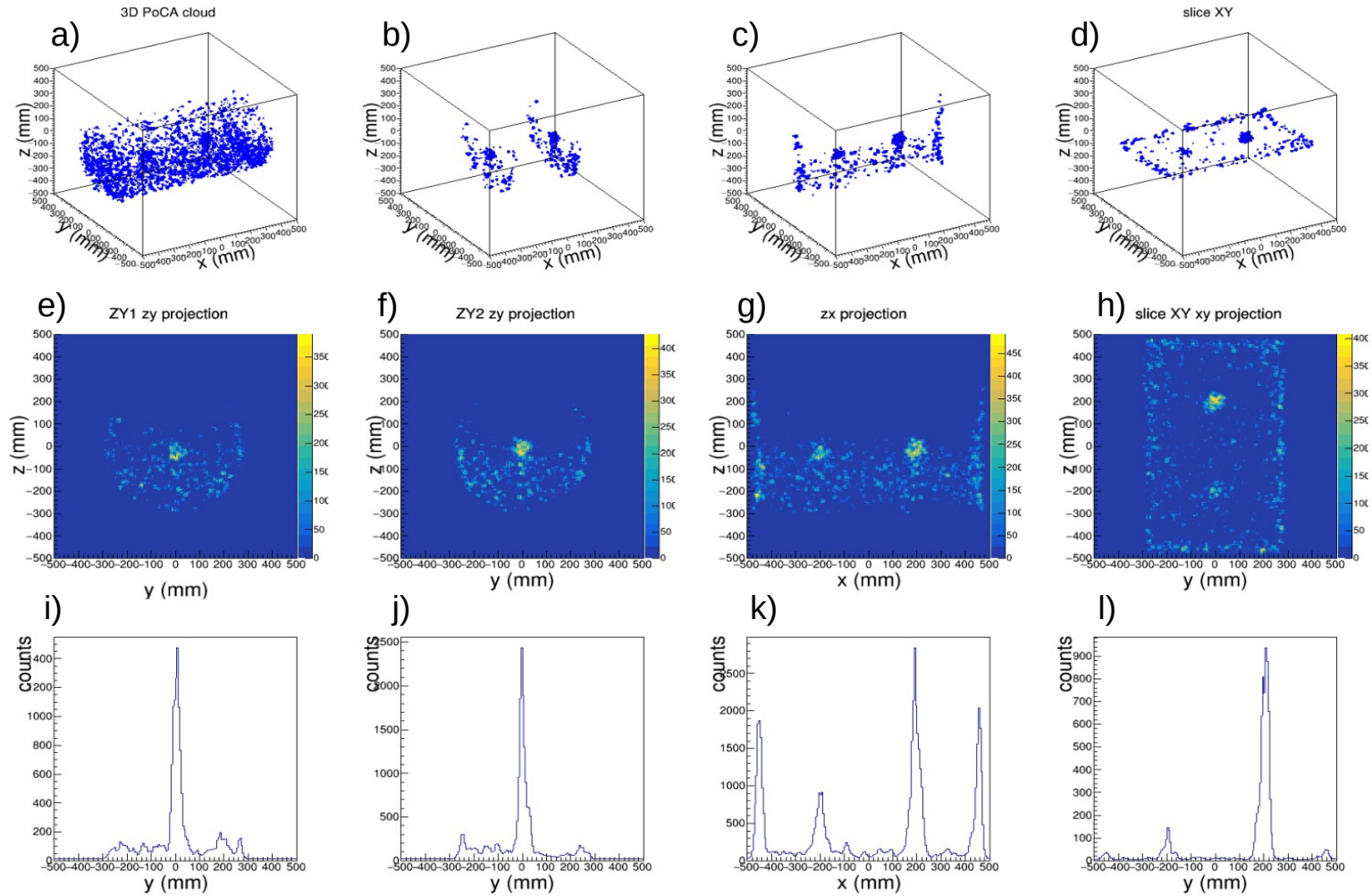
c)



d) Horizontal 100 mm slice of in the XY plane centered at the locations $x = 0$ cm were tungsten and lead targets are located.

d)

Applying cuts for removing background from concrete matrix



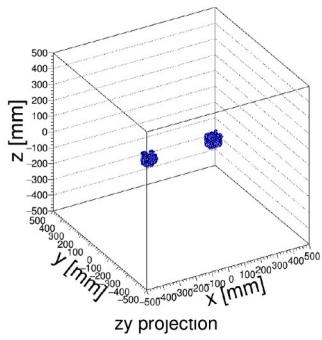
a). POCA reconstruction after applying clustering cut and median filtering.

b), c) and d) 100 mm slices after cut in the YZ,XZ an XY planes centered at target locations.

e), f), g) and h) 2D projections of 100 mm slices in the YZ,XZ an XY planes using ROOT data analysis package.

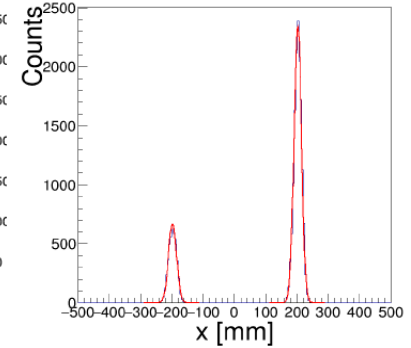
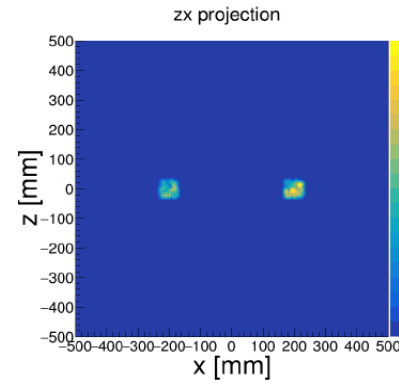
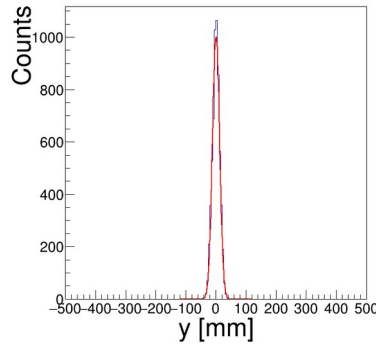
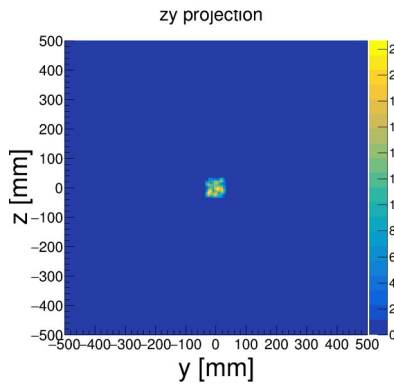
i), j), k) and l) 1D projections of 100 mm slices in the YZ,XZ an XY planes.

On all figures lead and tungsten targets are clearly reconstructed after removing background from concrete matrix.



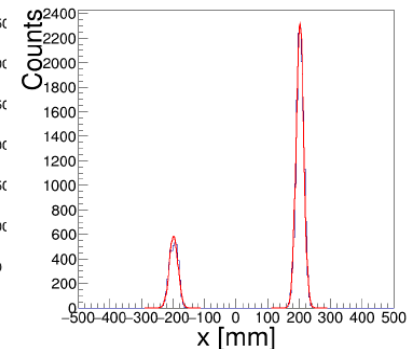
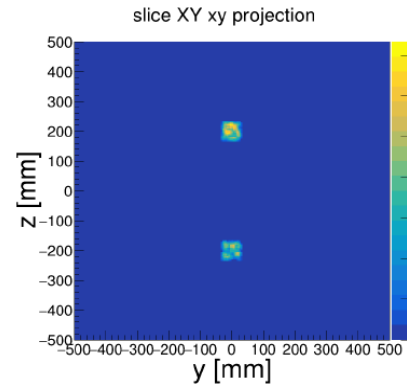
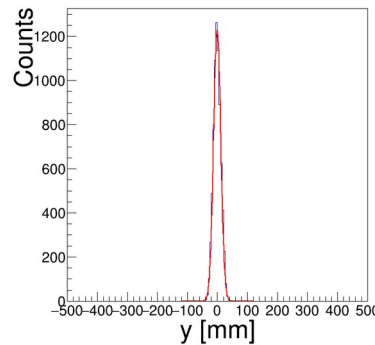
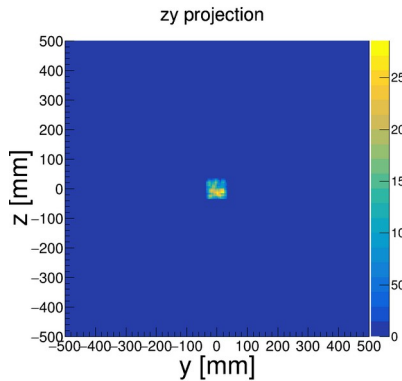
After combining XZ, ZY and XY slices two cube areas are finally cut from 3D PoCA image

Gaussian fits of 1D projections allow to localize lead and tungsten targets and the Gaussian area is a characterization of target material



2D and 1D **ZY1** projections of selected PoCA regions at position $x = -20$ cm

2D and 1D **ZX** projections of selected PoCA regions.

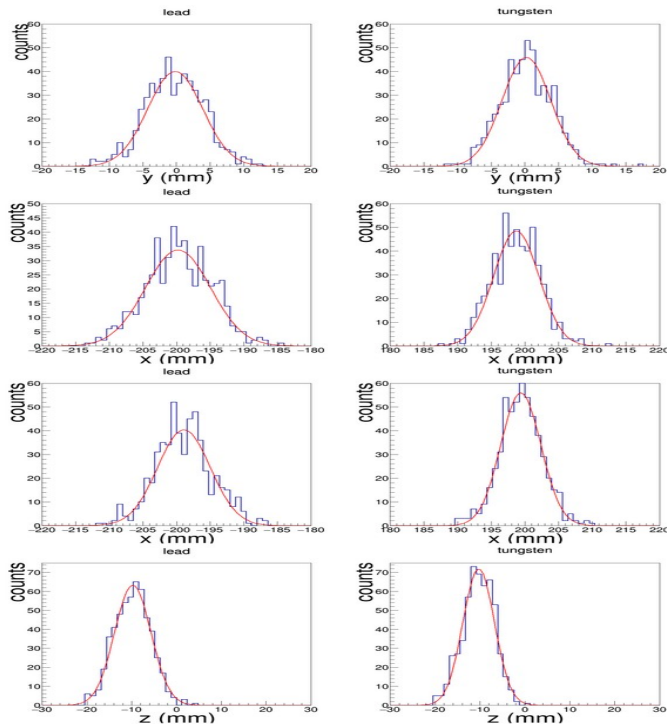


2D and 1D **ZY2** projections of selected PoCA regions at position $x = 20$ cm

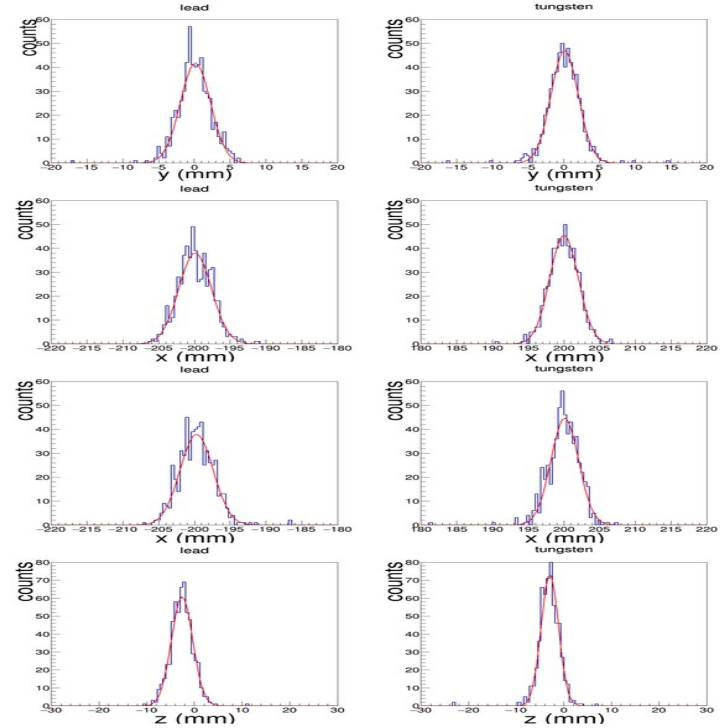
2D and 1D **XY** projections of selected PoCA regions.

Localization of material targets in both detector types

Planar type MTS: 2 tracking detectors



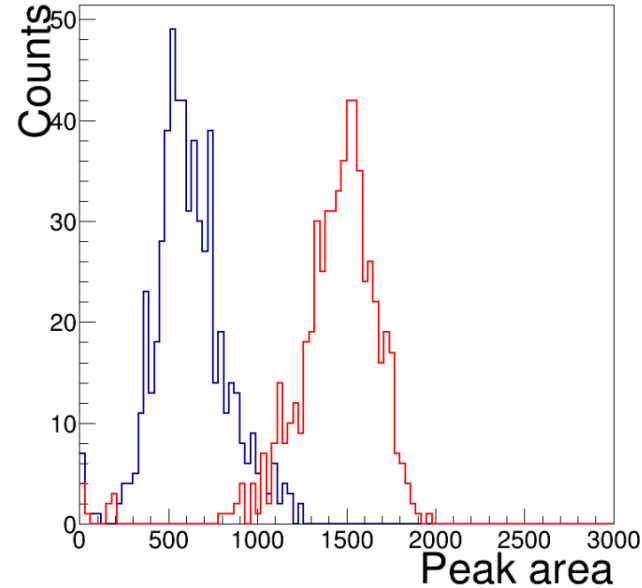
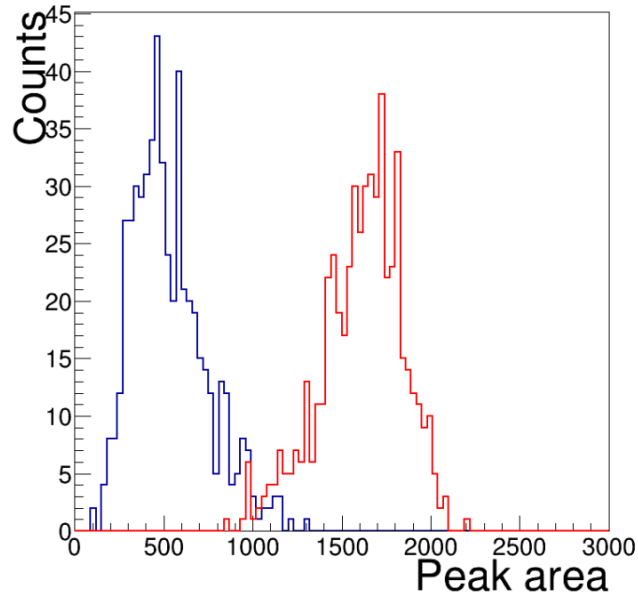
Tunnel type MTS: 4 tracking detectors



		Lead			Tungsten		
	x (mm)	y (mm)	z (mm)	x (mm)	y (mm)	z (mm)	
1 st scheme	-199 ± 5	-0.2 ± 4.2	-9.8 ± 4.1	199 ± 3	0.2 ± 3.6	-10.3 ± 3.8	
2 nd scheme	-199 ± 3	0.13 ± 2.1	-2.7 ± 2.2	200 ± 2	0.1 ± 1.9	-2.9 ± 2.3	

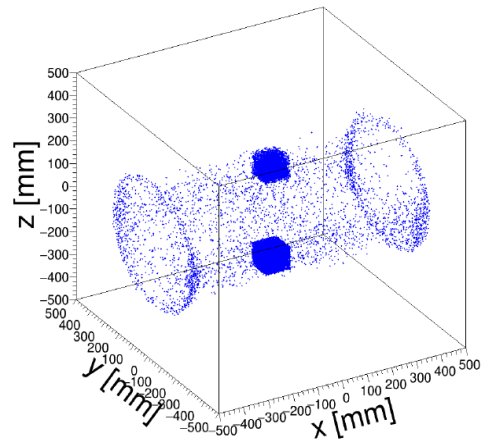
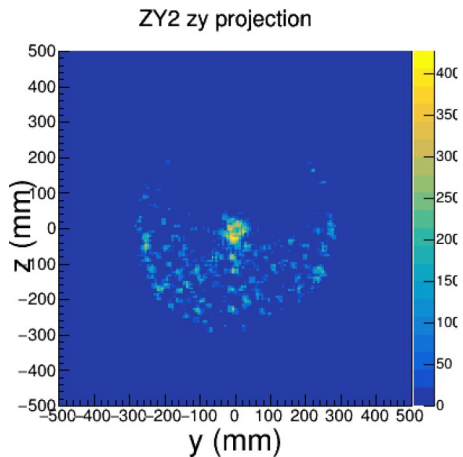
Cumulative distributions of reconstructed x,y,z coordinates for both detector types. Somewhat better performance demonstrate tunnel type detector scheme providing better localization in z coordinates and smaller deviations from mean due to better statistics from detected flux of inclined muons.

Possibility of material characterization

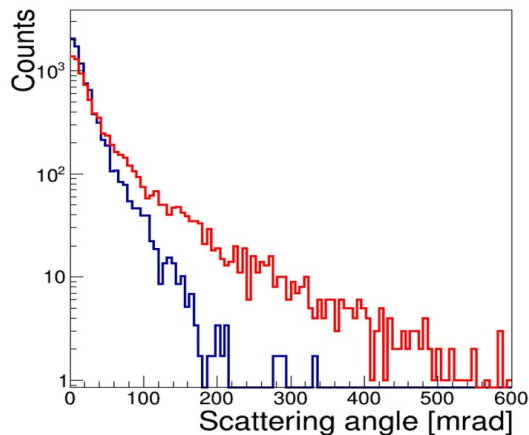


Distributions of Gaussian areas for lead (blue line) and tungsten (red line) plotted for 1st detector scheme (left) and 2nd one (right) representing material discrimination results for one hour measurement time.

Impact of concrete matrix on muon momentum and scattering angle distribution

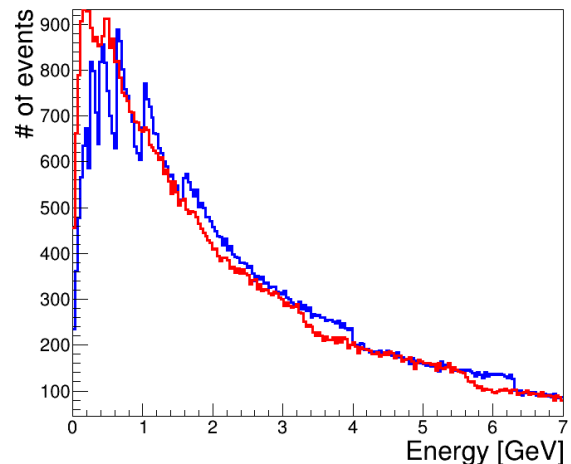


After applying the cuts the background from concrete matrix is removed only partially, except the lower part of the waste drum, which is a result of softening of muon spectrum and increasing muon scattering angle while passing concrete matrix.



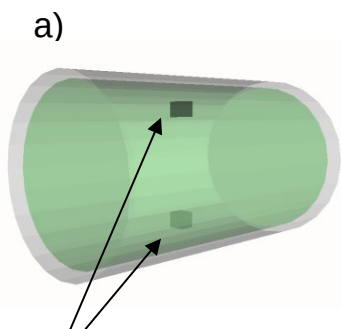
Scattering angles distribution for top (blue line) and bottom (red line) selected cube areas in PoCA cloud. Much more scattering point detected at the bottom part of waste drum.

Illustration of selection of cube-shaped areas of PoCA cloud at top and bottom of parts of waste drum.

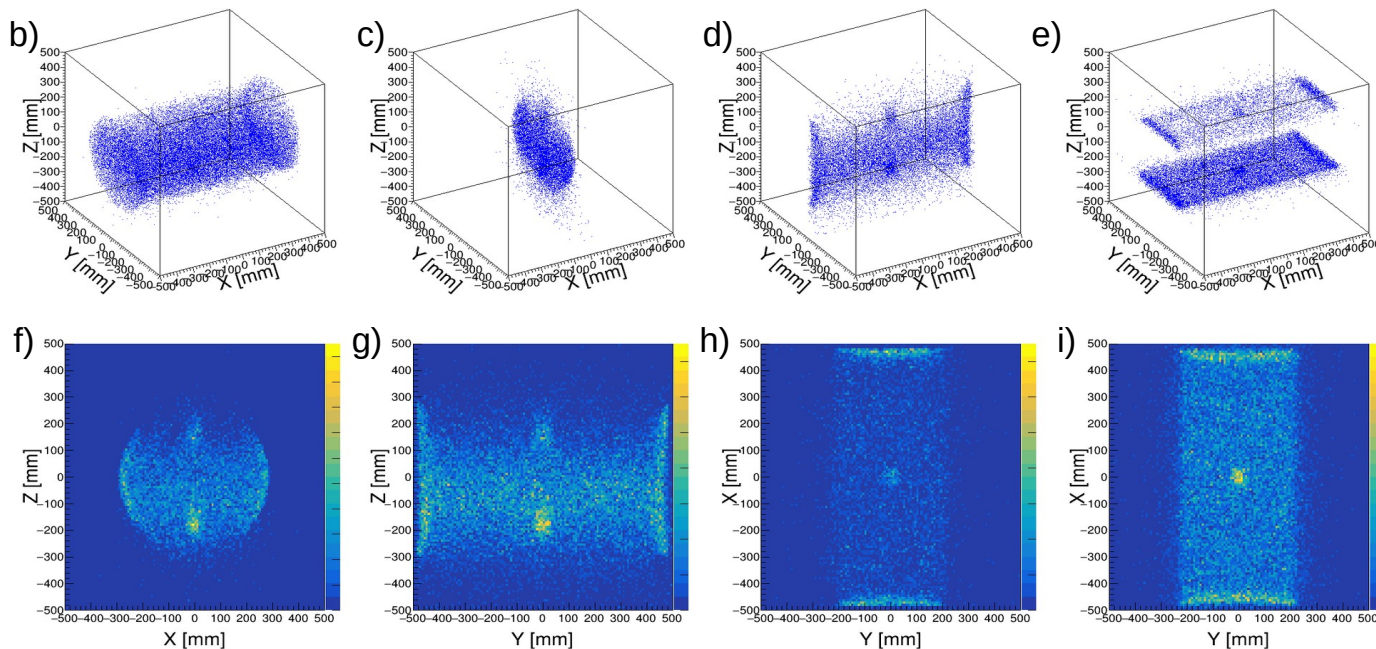


Energy spectra of muons hitting the top (blue line) detector plate and bottom (red line) detector plate. (the step feature of spectrum is a result of using tabulated data by CRY muon library.)

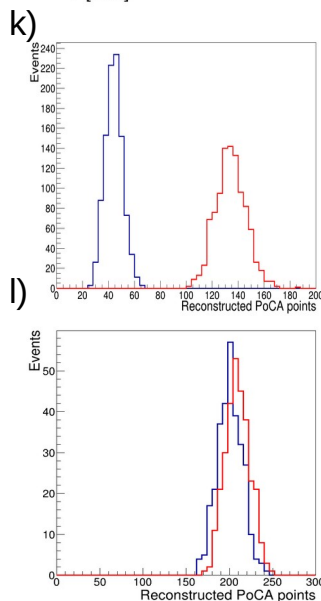
Impact of concrete matrix on material characterization



5 cm³ tungsten cubes located at positions z = 20 cm and z = -20 cm



- a). Illustration of positioning of two tungsten cubes
- b). Reconstructed PoCA image of waste drum
- c). ZY slice centered at location x = 0 cm.
- d). ZX slice centered at location y = 0 cm.
- e). XY slices centered at locations z = 20 cm and z = -20 cm.
- f). 2D projection of ZY slice
- g). 2D projection of XY slice at location z = 20 cm
- h). 2D projection of ZX slice at location z = -20 cm
- k) Reconstructed PoCA points for tungsten target at position z = 20 cm (blue color) and tungsten target at position z = -20 cm (red color) inside waste drum.
- l) Reconstructed PoCA points for tungsten target at position z = 20 cm (blue color) and tungsten target at position z = -20 cm (red color) without waste drum.



Results of simulation of two tungsten targets placed close to the top wall of the drum (z = 20 cm) and close to bottom wall (z = -20 cm) demonstrate that number of reconstructed PoCA points at the bottom position is much larger than that at the top position (see Figure k.). This effect relates to softening of muon spectrum due to muon energy loss in concrete matrix.

Conclusions and Summary

The performance of two detector schemes developed for the inspection of containers with conditioned nuclear waste using muon tomography was evaluated based on Monte Carlo simulations. As a quantitative measure for a comparative study of the two detector schemes, the localization accuracy of the high-Z material inside the nuclear waste drum was used.

The tunnel type detector showed better accuracy for high-Z material localization, but the planar type detector has similar performance in the case of good angular acceptance of cosmic ray muons.

It has been found that the number of reconstructed PoCA points depends on the location of the high-Z material in the concrete matrix of the container, which is the result of the softening of the cosmic muon spectrum due to energy losses during the passage of the concrete matrix. This effect must be taken into account for classification of high-Z materials detected in the containers with conditioned nuclear waste.